Modeling silicon spintronics

Viktor Sverdlov, Joydeep Ghosh, Dmitri Osintsev, and Siegfried Selberherr
Institute for Microelectronics, Technische Universität Wien
Gusshausstrasse 27–29, A-1040 Vienna, Austria
Email: {sverdlov|ghosh|osintsev|selberherr}@iue.tuwien.ac.at

***Abstract*— Silicon, the main material of microelectronics, is perfectly suited for spin-driven applications. All-electrical spin injection in silicon has been demonstrated, however, the magnitude of the corresponding signal is larger than theoretically predicted. We analyze the influence of electrostatic charge screening on the efficiency of spin injection at the ferromagnet-semiconductor interface. We show that the spin-injection efficiency cannot exceed the value obtained at the charge neutrality condition. Finally, we demonstrate that a large enhancement of the electron spin lifetime in silicon thin films can be obtained by applying shear strain, which is routinely used to boost the electron mobility in MOSFETs.**

***Index Terms*— Spin injection modeling, spin lifetime modeling, valley splitting modeling**

I. Introduction

Miniaturization of CMOS devices has made possible a tremendous increase in performance, speed, and density of modern integrated circuits. However, difficulties to reduce the supply voltage V_{DD} result in an approximately constant power dissipation per a single MOSFET. This leads to a rapid increase of generated heat with increasing transistor density, which results in a saturation of MOSFET miniaturization and puts limitations on the performance of integrated circuits. Therefore, research for finding alternative technologies and computational principles becomes urgently needed.

The MOSFET operation is fundamentally based on the charge degree of freedom of an electron. Another intrinsic electron property, the electron spin, attracts at present much attention as a possible candidate for complimenting or even replacing the charge degree of freedom in future electron devices.

Until recently, silicon was remaining aside from the main stream of spin-related applications: even a demonstration of basic elements necessary for spin related applications, such as injection of spin-polarized currents in silicon, spin transport, spin manipulation, and detection, was missing. The first demonstration of coherent spin transport through an undoped 350μm thick silicon wafer [1] has triggered a systematic study of spin transport properties in silicon [2]. The use of silicon for spin driven devices would greatly facilitate their integration with MOSFETs on the same chip.

II. Spin injection

Spin injection in silicon and other semiconductors by purely electrical means from a ferromagnetic metal electrode was not very successful until recently. The fundamental reason has been identified as an impedance mismatch problem [3]. A solution to the impedance mismatch problem is the introduction of a potential barrier between the ferromagnetic metal and the semiconductor [4]. A successful experimental demonstration of a signal which should correspond to spin injection in doped silicon at room temperature was first performed in 2009 [5] using an $Ni_{80}Fe_{20}/Al_2O_3$ tunnel contact. Electrical spin injection through silicon dioxide at temperatures as high as 500K has been reported in [6].

Regardless of a success in demonstrating spin injection at room temperature, there are unsolved challenges which may compromise the results obtained. According to theory, in a three-terminal scheme [2] the value of the voltage signal ΔV due to spin accumulation divided by the current density j flowing through the injecting contact is proportional to

$$\Delta V/j = P^2 \rho_S \sqrt{D_{DIFF}\tau_S}. \qquad (1)$$

Because of the injection and detection, the tunnel spin polarization P enters squared, and the silicon resistivity ρ_S multiplied with the spin diffusion length $l = \sqrt{D_{DIFF}\tau_S}$, where τ_S is the spin lifetime, determines the additional area resistance of the contact due to spin accumulation under it. However, there is a several orders of magnitude discrepancy between the signal measured and the theoretical value (1). It turns out that the signal is stronger in three-terminal measurements, while it is weaker in the non-local scheme [2]. The reasons for the discrepancies are heavily debated [7], [8] and it is apparent that more research is needed to resolve this controversy.

A. Spin injection in silicon through a space-charge layer

In a quite recent publication a ten-fold spin injection efficiency increase was predicted [9], which is attributed to electrostatic screening effects. In a conventional approach the presence of a space charge layer at the interface is ignored [10]. When the space charge layer is absent (charge neutrality), analytical expressions for the spin injection efficiency through a ferromagnetic-non-magnetic semiconductor interface can be obtained. The density of states in both materials is considered similar to avoid the impedance mismatch problem. When the charge current J_n flows through the junction, the spin accumulation in the semiconductor appears, which is characterized by the spin current J_s injection efficiency $\alpha = J_s/J_n$ and the spin density s injection efficiency $\beta = s/n$, where the carrier density n is equal to the doping level N_D under the charge neutrality conditions. The analytical expressions at the

This work is supported by the European Research Council through the grant #247056 MOSILSPIN.

ISBN: 978-1-61804-251-4

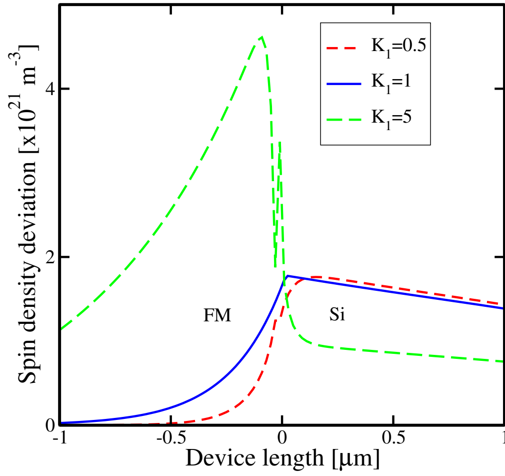

Fig. 1. Spin density distribution, when the charge current density is fixed to $23.4\,\mathrm{MA/m^2}$. $P = 0.2$. K_1 is the doping ratio in the ferromagnet to the non-magnetic material.

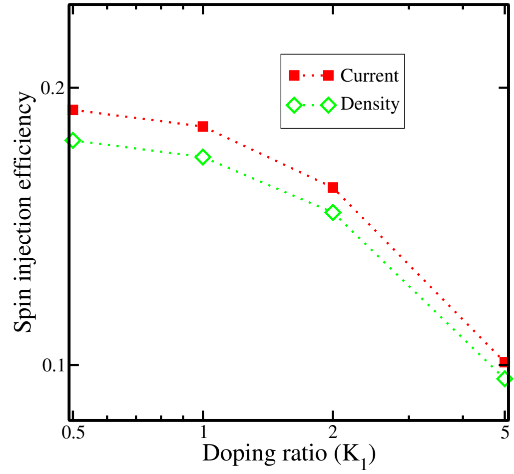

Fig. 2. Spin density and spin current injection efficiencies (α_D, and β_D), taken at the screening length λ_D away from the interface in the non-magnetic material, for $P = 0.2$.

Si interface for α and β are cumbersome. The simplified expressions, valid for small values of P, are written as:

$$\alpha = P\,\frac{l_d}{l_d + (1-P^2)\,l_u} \tag{2}$$

$$\beta = (1 - \frac{l_u}{l_d})\,\alpha \tag{3}$$

where $P = s/n$ is the equilibrium bulk spin polarization in the ferromagnet. The spin diffusion lengths $l_{u(d)}$ against (along) the electric field E are [10]

$$l_{u(d)} = \left(-(+)\frac{|eE|}{2k_BT} + \sqrt{\frac{|eE|}{2k_BT} + \frac{1}{l}}\right)^{-1}, \tag{4}$$

For the chosen current direction from the non-magnetic to ferromagnetic semiconductor, l_d is the spin diffusion length in the ferromagnet, while l_u is the length in the non-magnetic semiconductor. For simplicity the intrinsic spin diffusion length l is taken the same on both sides of the junction.

To violate the charge neutrality and introduce the space charge layer at the ferromagnetic-non-magnetic semiconductor interface, we modify the carrier concentration in the ferromagnet by assuming the ferromagnet to be doped to a concentration proportionally with a factor K_1 to the doping value N_D in the semiconductor. Thus, when K_1=1, the charge neutrality condition is recovered, while a charge accumulation and a charge depletion are introduced when K_1>1 and K_1<1, respectively, at the non-magnetic side of the junction. We investigate the carrier distribution and the spin current variation along the junction considering a fixed charge current density J_n=$23.4\,\mathrm{MA/m^2}$. The spin density s and the spin current J_s behave differently at the interface and in the bulk. When K_1>1 (K_1<1), s gradually piles up (drops down) in the bulk of the ferromagnet and drops down (piles up) in the bulk of the non-magnetic semiconductor (Fig.1), compared to the charge neutrality condition. This phenomenon happens due to the difference in the material conductivity proportional to the doping concentration, and the bulk electric field, which eventually modifies the effective spin diffusion length. On the contrary, when K_1>1 (K_1<1), s develops a dip (peak) at the ferromagnetic interface followed by a sharp peak (dip) at the non-magnetic semiconductor interface (Fig.1). These features are correlated with the charge depletion (accumulation) at the ferromagnetic/non-magnetic interface, which results in the formation of a potential profile with a barrier for electrons. These interface effects give rise to an alteration in the spin current at the interface, however persisting only up to the charge screening length (λ_D. The spin injection efficiencies at a distance λ_D away from the interface in the non-magnetic semiconductor displayed in Fig.2 shows an increment in both α_D, and β_D, compared to the charge neutrality case K_1 =1, if the spins are injected into a non-mgnetic material from the ferromagnet with doping level lower than in the non-magnetic material. However, its value is always limited by the bulk spin polarization of the ferromagnetic contact. Under similar conditions, the spin injection efficiency in the non-magnetic semiconductor bulk decreases, if the spins are injected from a highly doped ferromagnetic source.

III. Modeling Spin Relaxation

For a spin-based device the possibility to transfer the excess spin injected from the source to the drain electrode is essential. The excess spin is not a conserved quantity, in contrast to charge. While diffusing, it gradually relaxes to its equilibrium value which is zero in a non-magnetic semiconductor. In a ground breaking experiment it was demonstrated that spin can propagate through a 350μm silicon wafer at liquid nitrogen temperatures. A lower estimation for the spin lifetime at room temperature obtained within the three-terminal injection scheme was of the order 0.1-1ns [2]. This corresponds to an intrinsic spin diffusion length l=0.2-0.5μm. The spin lifetime is determined by the spin-flip processes. Several important spin relaxation mechanisms are identified [11], [12]. In silicon the spin relaxation due to the hyperfine interaction of spins with the magnetic moments of the ^{29}Si nuclei is important at low temperature. Because of the inversion symmetry in the

ISBN: 978-1-61804-251-4

silicon lattice the Dyakonov-Perel spin relaxation mechanism is absent in bulk systems [11], [12]. At elevated temperatures the spin relaxation due to the Elliot-Yafet mechanism [11], [12] becomes important.

The Elliot-Yafet mechanism is mediated by the intrinsic interaction between the orbital motion of an electron and its spin. Due to the spin dependence, the microscopic spin-orbit interaction does not conserve the electron spin, thus it generates spin flips, which is the Yafet process. When the microscopic spin-orbit interaction is taken into account, the Bloch function with a fixed spin projection is not an eigenfunction of the total Hamiltonian. Because the eigenfunction always contains a contribution with an opposite spin projection, even spin-independent scattering with phonons generates a small probability of spin flips, which is the Elliot process.

In order to analyze the spin relaxation in silicon, both, the Elliot and the Yafet processes must be taken on equal footing. In this way a good agreement between the experimentally observed and calculated spin life time as a function of temperature has been achieved confirming that in bulk silicon the Elliot-Yafet mechanism is the dominant spin relaxation mechanism at ambient temperatures [13]. The spin lifetime in undoped silicon at room temperature is about 10ns, which corresponds to a spin diffusion length of 2μm. In case of heavily doped silicon the spin lifetime is determined by the Elliot-Yafet mechanism due to ionized impurity scattering and is expected to be around 1ns at $N_D = 10^{19}\text{cm}^{-3}$, in agreement with experiments.

The main contribution to spin relaxation was identified to be due to optical phonon scattering between the valleys residing at different crystallographic axis, or f-phonons scattering [14], [15]. This scattering is enhanced at high electric field due to the accelerated f-phonon emission process to counteract a further deviation of the electron system from thermal equilibrium [16], which results in an unusual experimentally observed behavior, when the reduction of the carrier transition time between the injector and the collector is accompanied by a reduction in spin polarization.

The relatively large spin relaxation experimentally observed in electrically-gated lateral-channel silicon structures [17], [18] indicates that the extrinsic interface induced spin relaxation mechanism becomes important. This may pose an obstacle in realizing spin driven CMOS compatible devices, and a deeper understanding of fundamental spin relaxation mechanisms in silicon inversion layers, thin films, and fins is needed.

The theory of spin relaxation must account for the most relevant scattering mechanisms which are due to electron-phonon interaction and surface roughness scattering. In order to evaluate the corresponding scattering matrix elements, the wave functions must be provided.

To find the wave functions, we employ the Hamiltonian describing the valley pairs along the [001]-axis [19]. The Hamiltonian includes confinement, a spin-orbit effective interaction term with the effective constant Δ_{so}, and shear strain ε_{xy} entering with the deformation potential D_{xy}. It is possible to accurately describe the valley bulk dispersion in the presence of strain including shear strain dependent effective masses [20].

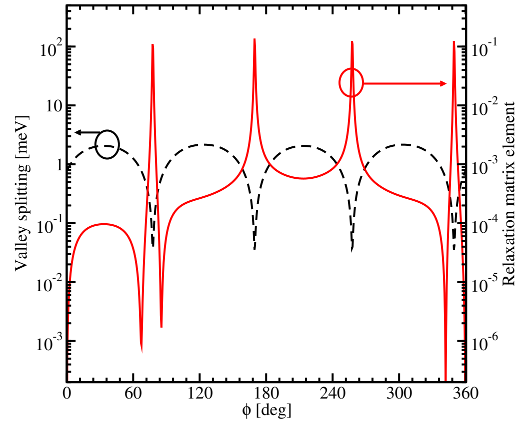

Fig. 3. Dependence of the normalized spin relaxation matrix elements and valley splitting on the angle between the incident and scattered waves for a quantum well of 4nm thickness, k_x=0.5nm^{-1}, k_y=0.1nm^{-1}, ε_{xy}=0.01%.

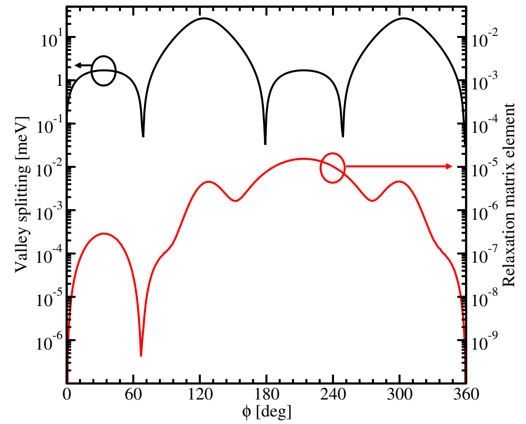

Fig. 4. Dependence of the normalized spin relaxation matrix elements and valley splitting on the angle between the incident and scattered waves for a quantum well of 4nm thickness, k_x=0.5nm^{-1}, k_y=0.1nm^{-1}, ε_{xy}=0.92%.

The Hamiltonian accounts for the unprimed subband (valley) splitting. In confined silicon systems it is usually assumed that the unprimed subbands, because they are originating from the two equivalent [001] valleys, are double degenerate. However, this is true only in the parabolic band approximation when the two valleys are independent. Due to the presence of the off-diagonal terms in the Hamiltonian, the [001] valleys are coupled, which results in an unprimed subband degeneracy lifting. In the case when the confinement potential is approximated with an infinite square well, the difference between the unprimed subband energies is as [19]

$$\Delta E = \frac{2y^2\sqrt{\Delta_{\text{so}}^2\left(k_{\text{x}}^2+k_{\text{y}}^2\right)+\left(D_{xy}\varepsilon_{\text{xy}}-\frac{\hbar^2 k_{\text{x}}k_{\text{y}}}{M}\right)^2}}{k_0 t\sqrt{\left(1-y^2-\eta^2\right)\left(1-y^2\right)}} \times \left|\sin\left(\sqrt{\frac{1-y^2-\eta^2}{1-y^2}}k_0 t\right)\right|, \tag{5}$$

with $y = \frac{\pi}{k_0 t}$, $\eta = \frac{m_l B}{k_0^2\hbar^2}$, t is the film thickness, and $k_0 = 0.15(2\pi/a)$ is the position of the valley minimum relative to the X-point.

The minimum of the $\sqrt{\ldots}$ term in (5) reveals a very strong increase of the intersubband spin relaxation shown in Fig.3.

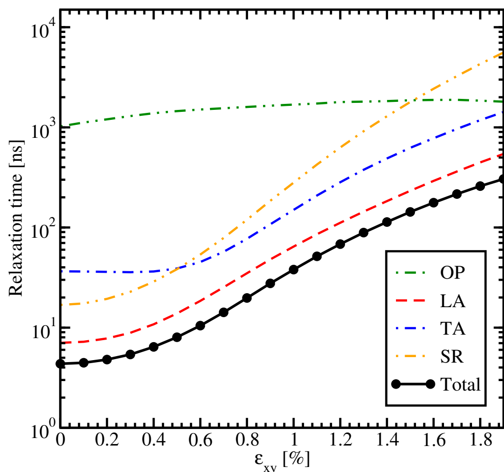

Fig. 5. Dependence of spin lifetime on shear strain for T=300K and a film of 4nm thickness. Optical (OP), longitudinal (LA) and transversal (TA) acoustic phonon, and surface roughness spin relaxation contributions are also shown.

Under these conditions the subband splitting is purely determined by the effective spin-orbit interaction term and is linear in $\Delta_{SO}\sqrt{k_x^2+k_y^2}$, where k_x, k_y are the components of the in-plane electron wave vector. This linear dependence of the splitting is similar to the Zeeman splitting in a magnetic field. Thus, the spin-orbit interaction term $\Delta_{SO}\mathbf{k}$ with $\mathbf{k}=(k_x,-k_y)$ can be interpreted as an effective magnetic field, while the pairs of states $(X_1,\uparrow),(X_{2'},\downarrow)$ and $(X_{2'},\uparrow),(X_1,\downarrow)$ it couples have similarities with the Zeeman spin-up, spin-down states split because of the effective field. Spin along the z-direction starts precessing in the in-plane effective field $\Delta_{SO}\mathbf{k}$, which results in a large mixing between the opposite spin states from the different valleys. This mixing results in large spin relaxation matrix elements defining hot spin relaxation spots seen in Fig.3. The origin of the spin relaxation hot spots in thin films lies in the unprimed subband degeneracy in a confined electron system. Because the hot spots are determined by the minimum of the $\sqrt{\dots}$ prefactor, they are located in the middle of the two-dimensional Brillouin zone in an unstrained film, thus contributing strongly to the spin relaxation.

When shear strain is applied, the spin relaxation hot spots are pushed towards higher energies and do not contribute significantly to spin relaxation. The minimum splitting between the subbands seen in Fig.4 does not result in any peculiarities of the spin relaxation matrix elements (Fig.4). We have checked that the valley splitting at the minima shown in Fig.4 is exactly zero. Thus the degeneracy between the subbands at these points is precisely recovered due to the oscillating $\sin\left(\sqrt{\frac{1-y^2-\eta^2}{1-y^2}}k_0 t\right)$ term. However, this degeneracy is insignificant, because it does not result in any peculiar behavior of the spin relaxation scattering matrix elements.

Moving the hot spots above the Fermi energy outside the occupied states region results in a sharp reduction of spin relaxation and in an increase of the spin lifetime with shear strain. Fig.5 demonstrates an order of magnitude enhancement of the spin lifetime at the stress values comparable achieved in advanced MOSFETs for boosting the electron mobility. Therefore, shear strain now routinely used to enhance the performance of modern MOSFETs can also be used to influence the spin propagation in the channel by enhancing the spin lifetime and the spin diffusion length significantly.

IV. Summary and Conclusion

Recent ground-breaking experimental and theoretical findings regarding spin injection and transport in silicon make spin an attractive option to supplement or to replace the charge degree of freedom for computations. The large discrepancy between the spin injection signal observed and predicted cannot be attributed to space charge effects. Mechanical stress routinely used to enhance the electron mobility can also be used to boost the spin lifetime.

Acknowledgment

This work is supported by the European Research Council through the grant #247056 MOSILSPIN.

References

[1] B. Huang, D. J. Monsma, I. Appelbaum, Coherent Spin Transport through a 350 Micron Thick Silicon Wafer, Phys. Rev. Lett. 99 (2007) 177209.
[2] R. Jansen, Silicon Spintronics, Nature Materials 11 (2012) 400–408.
[3] G. Schmidt, D. Ferrand, L. W. Molenkamp, A. T. Filip, B. J. van Wees, Fundamental Obstacle for Electrical Spin Injection from a Ferromagnetic Metal into a Diffusive Semiconductor, Phys. Rev. B 62 (2000) R4790–R4793.
[4] E. I. Rashba, Theory of Electrical Spin Injection: Tunnel Contacts as a Solution of the Conductivity Mismatch Problem, Phys. Rev. B 62 (2000) R16267–R16270.
[5] S. P. Dash, S. Sharma, R. S. Patel, M. P. de Jong, R. Jansen, Electrical Creation of Spin Polarization in Silicon at Room Temperature, Nature 462 (2009) 491–494.
[6] C. Li, O. van 't Erve, B. Jonker, Electrical Injection and Detection of Spin Accumulation in Silicon at 500K with Magnetic Metal/Silicon Dioxide Contacts, Nature Communications 2 (2011) 245.
[7] R. Jansen, A.M. Deac, H. Saito, S. Yuasa, Injection and Detection of Spin in a Semiconductor by Tunneling via Interface States, Phys. Rev. B 85 (2012) 134420.
[8] Y. Song, H. Dery, A. Lemaitre, Magnetic-Field-Modulated Resonant Tunneling in Ferromagnetic-Insulator-Nonmagnetic Junctions, Phys. Rev. Lett. 113 (2014) 047205.
[9] M.R. Sears, and W.M. Saslow, Spin Accumulation at Ferromagnet/Nonmagnetic Material Interfaces, Phys. Rev. B 85 (2012) 014404.
[10] Z.G. Yu, and M.E. Flatte, Spin Diffusion and Injection in Semiconductor Structures: Electric Field effects, Phys. Rev. B 66 (2002) 235302.
[11] J. Fabian, A. Matos-Abiaguea, Ch. Ertlera, P. Stano, I. Zutic, Spintronics: Fundamentals and Applications, Rev. Mod. Phys. 76 (2004) 323–410.
[12] I. Zutic, J. Fabian, S. Das Sarma, Semiconductor Spintronics, Acta Phys. Slovaca 57 (2007) 567–907.
[13] J. L. Cheng, M. W. Wu, J. Fabian, Theory of the Spin Relaxation of Conduction Electrons in Silicon, Phys. Rev. Lett. 104 (2010) 016601.
[14] P. Li, H. Dery, Spin-Orbit Symmetries of Conduction Electrons in Silicon, Phys. Rev. Lett. 107 (2011) 107203.
[15] Y. Song, H. Dery, Analysis of Phonon-Induced Spin Relaxation Processes in Silicon, Phys. Rev. B 86 (2012) 085201.
[16] J. Li, L. Qing, H. Dery, I. Appelbaum, Field-Induced Negative Differential Spin Lifetime in Silicon, Phys. Rev. Lett. 108 (2012) 157201.
[17] J. Li, I. Appelbaum, Modeling Spin Transport in Electrostatically-Gated Lateral-Channel Silicon Devices: Role of Interfacial Spin Relaxation, Phys. Rev. B 84 (2011) 165318.
[18] J. Li, I. Appelbaum, Lateral Spin Transport through Bulk Silicon, Appl. Phys. Lett. 100 (16) (2012) 4704802.
[19] D. Osintsev, O. Baumgartner, Z. Stanojevic, V. Sverdlov, S. Selberherr, Subband Splitting and Surface Roughness Induced Spin Relaxation in (001) Silicon SOI MOSFETs, Solid-State Electronics 90 (2013) 34 – 38.
[20] V. Sverdlov, Strain-Induced Effects in Advanced MOSFETs, Springer, Wien - New York, 2011.